

Simulations with solution based mesh adaptation for fluid structure interactions

J.J.H.M. Sterenberg¹⁾, A.H. van Zuijlen²⁾, H. Bijl³⁾

¹⁾ PhD-researcher, ²⁾ Assistant professor, ³⁾ Full professor

Technical University of Delft, Department of Aerodynamics, the Netherlands

ABSTRACT

Simulations of multi-physics systems are time consuming and therefore acceleration techniques are commonly used. The current research focuses on the application of solution based mesh adaptation to fluid structure interaction (FSI) computations. The FSI-solver used in this work is a partitioned solver that consists of a RANS solver for the flow and a rigid body solver for the structure. The aim is to assess the gain in efficiency when using solution based mesh adaptation in combination with FSI. Thereby, the number of time steps between successive adaptations and the number of adaptation steps per adaptation are considered. Preliminary results indicate the potential of the method, since flow features are resolved more detailed with the same number of cells.

KEYWORDS

Fluid Structure Interactions, Unsteady solution based mesh adaptation, RANS

1 INTRODUCTION

It is well known that for a correct and efficient design of flexible structures, fluid structure interactions should be considered. This is one of the current issues in the field of wind energy, since due to the increased size of wind turbines blades, flexibility issues are non-negligible.

Although the computer capacity has improved, the simulations of fluid structure interaction systems require large computational times and are inherently expensive. Therefore, more research is needed to find options to reduce the computational times of such simulations. Since for (un)steady computations it is proven that solution based mesh adaptation increases the efficiency [1], it is investigated if the application of unsteady solution based mesh adaptation to FSI computations also leads to an increase in efficiency.

2 MESH ADAPTATION FOR FSI

2.1 Unsteady solution based mesh adaptation

Mesh adaptation concerns the modification of an existing mesh with the aim to increase the computational efficiency and accuracy. The modifications can be based on a known solution on the current mesh, such that regions where small scale flow features are present will be refined and regions where only large scale features are present will be coarsened. In this way, with a reduced number of cells it is possible to maintain the accuracy of the solution and a gain in efficiency should therefore be possible.

Drawback is that the modification of the mesh increases the computational time. This means that the application is only advantageous when the efficiency gain by the cell reduction exceeds the reduction in efficiency due to the re-meshing. For unsteady computations, it is therefore not trivial that the most beneficial solution is to adapt the mesh each time step.

The solution based mesh adaptation is based on error indicators that are a measure of the discretization error. In this work, for all cell faces the \log_2 value of the error indicator is computed and stored in bins [2]. Depending on the threshold value for refinement/coarsening, all cells in a particular bin can be flagged for adaptation. The \log_2 scaling prevents over-refinements of regions where severe flow features are present and the consequence that other important flow features are not resolved properly. Furthermore, it enables to compute threshold values based on the target number of cells after adaptation, since an estimate of the number of cells after adaptation can be made a priori.

The error indicator is a finite difference formulation based on one or more flow variables, multiplied by a factor which is based on the spatial resolution. In the preliminary computations the pressure gradient is taken as sensor and the error indicators are defined by:

$$\varepsilon = \Delta \left(\|\nabla p\| \right) \cdot h_{sd}^x \quad (1)$$

In this equation ∇p is the pressure gradient, h_{sd} is the minimum distance between the face and the neighbouring cell centers and x is a power term for the distance. The minimum distance h_{sd} is used to prevent over-refinements by an underestimation of the error indicator in case large cell size jumps occur. Thereby, for small values of x the adaptations are

performed locally, whether for large values of x more global adaptations are allowed. A value of $x = 1.5$ is established to give the most satisfying results [3],[4].

For now, in this preliminary work only refinements are possible. Unsteady simulations have been performed, where the average of error indicators over a time period is used to perform one adaptation sequence. Subsequently, the same computation is executed again with the new mesh. In order to have an adaptation algorithm that can be applied more efficiently to unsteady flows, coarsening must be available as well. Currently, coarsening is being implemented.

2.2 FSI solver

For the flow, a Reynolds Averaged Navier Stokes (RANS) solver in combination with the one equation Spalart Allmaras turbulence model is used. The structure is assumed rigid, which simplifies the structural model to a system of equations of motion. The FSI solver is of the partitioned type, meaning the flow and structure are solved subsequently. In this work, the structure and the flow are solved only once per time step (loosely coupled). This reduces the computational time, but is less accurate. The mesh movement is performed by making use of Radial Basis Function (RBF), to determine the flow-structure interface displacements.

3 TEST CASE: VISCEL

The test case is derived from the VISCEL project part II [5]. A rigid NACA 0012 airfoil section is modelled that can move in the chord wise direction (edge wise) and in the direction perpendicular to it (flap wise). In Figure 1 a schematic overview is presented of the structural model.

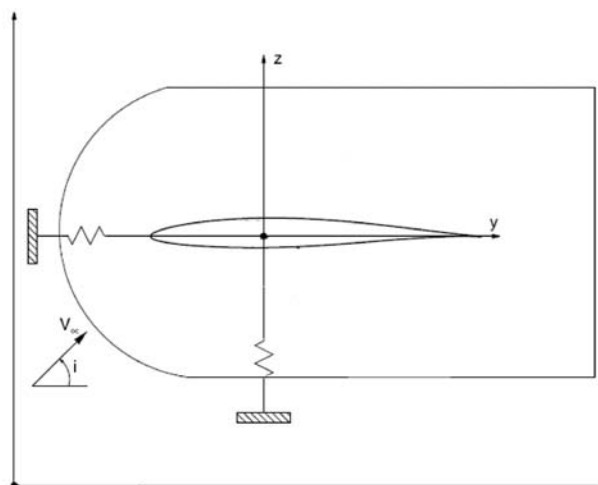


Figure 1: Structural model

The equations of motion for this system are given by:

$$\begin{bmatrix} \rho_s & 0 \\ 0 & \rho_s \end{bmatrix} \begin{Bmatrix} \ddot{y} \\ \ddot{z} \end{Bmatrix} + \begin{bmatrix} k_y & 0 \\ 0 & k_z \end{bmatrix} \begin{Bmatrix} y \\ z \end{Bmatrix} = \frac{1}{2} \rho_a \bar{V}^2 c \begin{Bmatrix} f_y \\ f_z \end{Bmatrix}, \quad (2)$$

where f_y and f_z are aerodynamic coefficients, (\cdot) is differentiation with respect to the time and all the other variables are presented in Table 1 and Table 2. Furthermore, the structural stiffnesses k_y and k_z are defined by:

$$\begin{aligned} k_y &= \rho_s \omega_y^2, \\ k_z &= \rho_s (\omega_z^2 + \Omega^2). \end{aligned} \quad (3)$$

The variables ω_y and ω_z are the natural frequencies in the edge wise and flap wise direction and Ω represents the rotational velocity of the rotor.

Table 1: Settings flow solver

Parameter	Used Settings
Initial angle of attack α_0	18°
Initial y-position y_0	0 m
Initial z-position z_0	0 m
Initial y-velocity \dot{y}_0	0 m/s
Initial z-velocity \dot{z}_0	0 m/s
Reynolds number Re_c	2×10^6
Ambient pressure p	101325 Pa
Kinematic viscosity ν	$1.716 \times 10^{-5} \text{ m}^2/\text{s}$
Density ρ_a	1.224 kg/m ³
Undisturbed flow velocity \bar{V}	34.32 m/s
Mach number Ma	0.1
Ratio spalart viscosity and kinematic viscosity $\tilde{\nu}/\nu$	0.1
Chord c	1 m

Table 2: Settings structure solver

Parameter	Used Settings
Mass ρ_s	61.2 kg
Stiffness in y-direction k_y	35321.938 N/m
Stiffness in z-direction k_z	12254.480 N/m

4 CONCLUSIONS

Results will be presented that follow from the preliminary work where only refinements are possible. Since no proper benchmark case is available yet, a qualitative review is given. Considered are two vorticity plots: one is for a manually made grid with 65k cells, the other is for a 32k mesh that is adapted (2x) to a 65k mesh. The adaptation is based on the largest error indicators of a FSI computation of 1 second physical time. In Figure 2 the two vorticity plots are given for $t = 0.27s$.

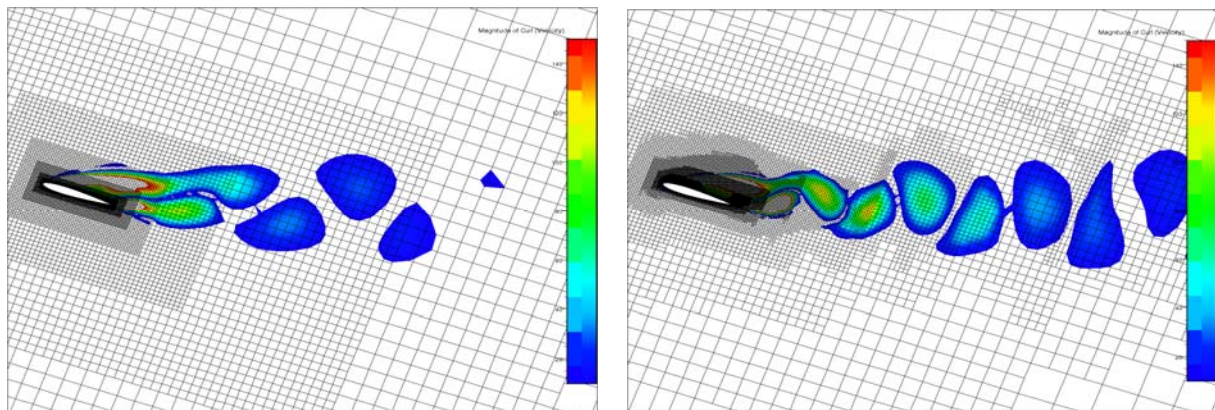


Figure 2: Differences in the solution between an non-adapted (left) and adapted grid (right) of both 65k cells

Three important aspects can be seen in figure 2. Firstly, it can be seen that the strength of the vorticity is better preserved in case the adapted grid is used. Secondly, flow details are better resolved for the adapted grid. Thirdly, the adapted regions can be seen clearly: close to the airfoil and in the wake area adaptations are performed.

The preliminary results are promising and therefore the adaptation routine is currently extended with coarsening capabilities in order to make it able to perform multiple adaptations during the unsteady computation.

BIBLIOGRAPHY

- [1] Gardner, A., Richter, K. and Rosemann, H., "Simulation of Oscillating Airfoils and Moving Flaps Employing the DLR-TAU Unsteady grid adaptation", New Results in Numerical and Experimental Fluid Mechanics VI, pp 170-177, Vol. 96/2008, 2007.
- [2] Aftosmis, M. and Berger, M., "Multilevel Error Estimation and Adaptive h -refinement for cartesian Meshes with embedded boundaries", AIAA, Vol. 2002-0863, 2002.
- [3] Lucas, P., "An automated approach to optimize numerical accuracy for a given number of grid cells applied to Cartesian grids", Master's thesis, Delft University of Technology, 2005, http://www.aero.lr.tudelft.nl/education/pdf/2005_1_03.pdf.
- [4] Lucas, P., "An automated approach to optimize numerical accuracy for a given number of grid cells applied to Cartesian grids", Submitted to: International journal for numerical methods in fluids, 2006.
- [5] Chaviaropoulos, P. et al., "Viscous and aeroelastic effects on wind turbine blades: VISCEL project partII", Wind Energy, 2003.